International Journal of Automotive Technology, Vol. 1, No. 1, pp. 26–34 (2000)

1229-9138/2000/001-04

HYDROPLANING ANALYSIS BY FEM AND FVM – EFFECT OF TIRE ROLLING AND TIRE PATTERN ON HYDROPLANING

Y. NAKAJIMA*, E. SETA, T. KAMEGAWA and H. OGAWA

Bridgestone Corporation 3-1-1, Ogawahigashi-Cho, Kodaira-Shi, Tokyo 187-8531, Japan

(*Received 12 June 2000*)

ABSTRACT–The new numerical procedure for hydroplaning has been developed by considering the following three important factors; fluid/structure interaction, tire rolling, and practical tread pattern. The tire was analyzed by FEM with Lagrangian formulation and the fluid is analyzed by FVM with Eulerian formulation. Since the tire and the fluid are modeled separately and their coupling is automatically computed by the coupling element, the fluid/structure interaction of the complex geometry such as the tire with the tread pattern can be analyzed practically. We verified the predictability of the hydroplaning simulation in the different parameters such as the water flow, the velocity dependence of hydroplaning, and the effect of the tread pattern on hydroplaning. In order to predict the streamline in the contact patch, the procedure of the global-local analysis was developed. Since the streamline could be predicted by this technology, we could develop the new pattern in a short period based on the principle; "make the stream line smooth".

KEY WORDS : Hydroplaning, Fluid/Structure interaction, FEM, FVM

1. INTRODUCTION

The hydroplaning is one of the most important performances to design the tread pattern of a tire, because a vehicle will lose its controllability once it occurs. So many engineers and researchers have studied the hydroplaning phenomena. The effects of many factors on hydroplaning were investigated in experimental works, such as road texture, inflation pressure, tire velocity, tread pattern, load and water depth etc (Albert, and Walker, 1965; Albert, 1968; Yeager and Tuttle, 1972; Horner and Joyner, 1970; Browne, 1975). In the most of analytical works, hydroplaning was solved by the 2D Reynolds equation and the fluid/structure interaction was considered in some of them (Browne and Whicker, 1997; Browne et al., 1972, 1975; Browne, 1977a, 1977b; Hays and Browne, 1974; Moore, 1964, 1965, 1967, 1975; Rohde, 1977; Whicker et al., 1976; Agrawall and Henry, 1980; Sakai, 1987; Boness 1968). CFD was also applied to analyze the 2D Reynolds equation including the fluid/structure interaction (Okamura and Someya, 1977a, 1977b). Furthermore in the recent years 3D-CFD has been performed, in which hydroplaning was solved by the Navier-Stokes equation including the free surface and the turbulence model (Grogger and Weiss, 1996, 1997).

Though there are a few researchers who solved the hydroplaning phenomena by the FEM, the FEM have not been popular for the hydroplaning study. Because it was difficult to consider the three important factors in the FEM. Three factors are the fluid/structure interaction in 3D models, tire rolling and complicated tread pattern geometry, which are necessary for tread pattern design if we use the hydroplaning simulation as the tire design tool. Though the fluid/structure inter- action was considered in the hydroplaning simulation (Okamura and Someya, 1977a, 1977b; Grogger and Weiss, 1996, 1997), other two factors have not been considered.

So our motivation was to establish the new numerical procedure for hydroplaning in which the three important factors were considered. This paper describes how to consider the three important factors and how to apply this technology to practical tread pattern design.

2. MECHANISM OF HYDROPLANING

The hydroplaning is a hydrodynamic phenomenon caused by the collision of water to a tire at high speed. The separation of the tire and the road due to the colli-

* *Corresponding author.* e-mail: nakajl-y@bridgestone.co.kr

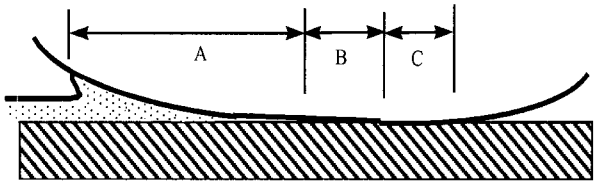

Figure 1. Three zone concept of hydroplaning (1).

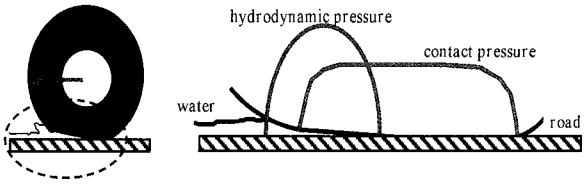

Figure 2. Schematic figure of dynamic hydroplaning.

sion leads to the reduction of the wet performance of a tire. The hydroplaning is usually explained by the well-known three zone concept as shown in Figure 1 (Albert and Walker, 1965; Moore, 1965; Hays and Browne, 1974). In the A region, the tire floats on thick water films and the water wedge penetrates into the contact patch so that the tire is fully separated from the road. In the B region, the tire is on thin water films. This is the transition region from floating to contact. In the C region, the tire contacts with the road completely.

The hydroplaning is classified into two kinds of phenomena (Moore, 1965). One is the dynamic hydroplaning. When a vehicle drives into thick water films at high speed, the hydrodynamic pressure is generated by the inertia of water and the tire floats on the water films. The other is the viscous hydroplaning. When a vehicle drives on thin water films, the hydrodynamic lubrication between the tire and the road surface occurs by the viscous effect, and then the tire slips on the wet road. The dynamic hydroplaning has the dominant effect in the A region. On the other hand, the viscous effect has the dominant effect in the B region.

Though both the inertia and the viscosity are important for hydroplaning, we just focused the aim of the simulation on dynamic hydroplaning in this study. One of reasons is that the 10 mm depth of water films, which is the measurement condition of the hydroplaning velocity in this study, is thick enough for the dynamic hydroplaning to be dominant. The important aspects of the dynamic hydroplaning of pneumatic tires can be satisfactorily explained on a purely inertial basis. NASA's hydroplaning velocity prediction formula (Homer and Joyner, 1970), derived solely on the basis of nonviscous flow, should be given great credence. Viscous effects need to be considered only if a detailed analysis of the fluid flow is desired (Browne et al., 1972). The other reason is that the road surface property of micro-texture may be considered to be effective in the 'thin film' penetration region of the ground contact.

Sharp points in the road surface will penetrate to and into the rubber surface and the effective friction developed will contain some component due to the shear of the rubber at these points. The micro-texture defines its inherent frictional characteristics (Albert and Walker, 1965). Because of these reasons, the viscous hydroplaning is considered to be less important than the dynamic hydroplaning in this study.

The schematic figure of dynamic hydroplaning is shown in Figure 2 and the mechanism of hydroplaning on thick water films is the following:

(1) Water collides with a tire at high speed;
(2) Hydrodynamic pressure is generated by the inertia of water;
(3) When the hydrodynamic pressure exceeds the contact pressure at the leading edge, the tire starts floating on water;
(4) Tire deformation due to the hydrodynamic pressure increases progressively;

Due to this deformation the wedge of water films penetrates into the contact patch, the depth of water and the hydrodynamic pressure increase progressively. Since hydroplaning includes the fluid/structure interaction, both tire deformation and fluid flow must be simultaneously simulated.

3. GOVERNING EQUATIONS

Since we focused the aim of this study on the dynamic hydroplaning, we ignored the viscosity of water. So the governing equations of fluid becomes the Eulerian equations as follows:

mass conservation

$$\int_V \frac{\partial \rho}{\partial t} dV = -\int_S \rho \mathbf{u} \cdot \mathbf{n} dS \tag{1}$$

momentum conservation

$$\int_V \frac{\partial (\rho \mathbf{u})}{\partial t} dV = -\int_S (\rho \mathbf{u})(\mathbf{u} \cdot \mathbf{n}) dS + \int_S \mathbf{T} \cdot \mathbf{n} dS \tag{2}$$

energy conservation

$$\int_V \frac{\partial e_t}{\partial t} dV = -\int_S e_t \mathbf{u} \cdot \mathbf{n} dS + \int_S \mathbf{u} \cdot \mathbf{T} \cdot \mathbf{n} dS \tag{3}$$

where ρ is the density, $\mathbf{u}$ is the velocity of fluid, $\mathbf{T}$ is the stress tensor of fluid force, and e_t is the inter-

nal energy. Since the viscosity of water is ignored, the viscous hydroplaning in the B region is not considered in this study.

4. DIFFICULTIES IN HYDROPLANING SIMULATION

There are two difficulties in the hydroplaning simulation. One is the fluid/structure interaction in a rolling tire. If we simulate the hydroplaning by Lagrangian formulation, mesh of water are largely distorted due to the tire rolling, particularly meshes in the lateral grooves of the tire model are severely distorted as shown in Figure 3. Furthermore, meshes of water in the contact area are largely deformed so that the thickness of the mesh will become too small to continue the calculation.

The deformable Eulerian mesh such as ALE method (MSC. Dytran) is often used to solve such problems due to large deformation and distortion. But the volume of the fluid region in the contact area disappears while the tire is loaded, so it is very difficult that we calculate the fluid flow in the contact area by ALE. There is the possibility that hydroplaning can be solved by ALE with remeshing. But many remeshing procedures of the fluid region are required during a very short time step (which is about 0.1-1msec), so hydroplaning simulation by ALE with remeshing is impractical.

The other difficulty in the hydroplaning simulation is the meshing problem in the fluid region when the practical tread pattern is considered. Since the practical tread pattern has the complicated geometry as shown in Figure 4, it is difficult to generate the compatible mesh between the practical tread pattern and the fluid region. Furthermore the distortion of the fluid mesh shown in Figure 3 becomes severer when the practical tread pattern is considered. Hence, the new procedure that can simulate hydroplaning with practical tread pattern is required.

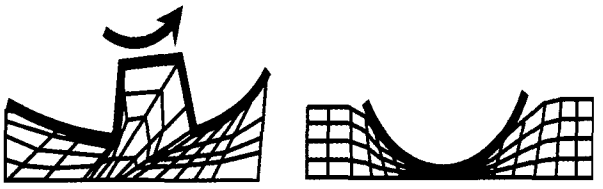

Figure 3. Difficulty in hydroplaning simulation.

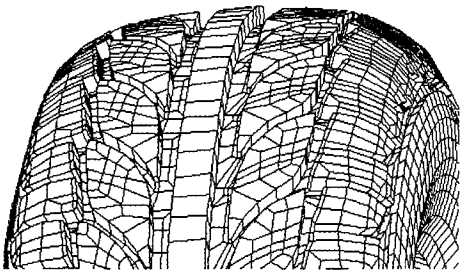

Figure 4. Practical tire tread pattern.

5. MODELING OF TIRE AND FLUID

In order to solve the aforementioned problems, we used the commercial explicit code MSC.Dytran in which the tire is analyzed by FEM (Finite Element Method) with Lagrangian formulation and the fluid is analyzed by FVM (Finite Volume Method) with Eulerian formulation. Furthermore the interface between the tire and the fluid is modeled by the general coupling, which is the special function in MSC.Dytran, in order to consider the fluid/structure interaction as shown in Figure 5.

The general coupling is very useful for Euler-Lagrange coupling. The features are the followings (MSC. Dytran);

(1) Lagrangian elements for structure and Eulerian elements for fluid are modeled separately, and the interface of them is modeled as coupling elements;
(2) The general coupling function computes the interaction between the Lagrangian mesh and the Eulerian mesh and enables complex fluid-structure interaction problems to be analyzed;
(3) The coupling elements, which are generated on the surface of the Lagrangian mesh, transfer the forces between the two solvers;
(4) The surface acts as a boundary to the flow of water in the Eulerian mesh. At the same time, the fluid pressure in the Eulerian elements causes forces to act on the coupling surface, and the forces causes deformation of the Lagrangian elements;
(5) Deformation of the fluid mesh does not occur. The forces of the fluid/structure interaction are transferred by the coupling elements, and the coupling elements, which are not compatible with the fluid mesh, overlap in the fluid domain;

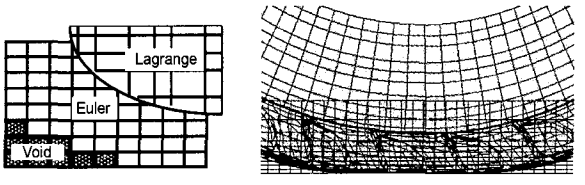

Figure 5. General coupling and modeling of tire and fluid.

Since the fluid is analyzed by Eulerian formulation, deformation of the fluid mesh does not occur even if that of the structural mesh occurs. Hence the complex fluid/structure interaction problems, hydroplaning simulations of tires with practical tread pattern for example, can be analyzed practically when we use this function.

The free surface is modeled by the volume fraction of water. If an element is completely filled with water, the volume fraction of water is 1.0. Otherwise if an element is completely empty, the volume fraction of water is 0. Propagation of the volume fraction of water is solved by the transport equation (MSC. Dytran).

The overlapping appearance of the tire model in the fluid domain is shown in Figure 5. The coupling elements are modeled on the surface of the tread pattern. The fluid domain is large enough to transport water when the free surface moves.

6. HYDROPLANING ANALYSIS OF TIRE WITH PATTERN

The result of the hydroplaning analysis of the tire with tread pattern is shown in Figure 6. The velocity of the tire is 60km/h, the tire size is 205/55R16, the inflation pressure is 220kPa, and the load is 4,500 N. The number of elements of the fluid domain is almost 39,000 that include the number of the coupling elements, and the number of elements of the tire is almost 18,000. Prescribed velocities are applied to the tire model in the horizontal and rotational direction. Friction coefficient between the tire and the road is 0. The size of

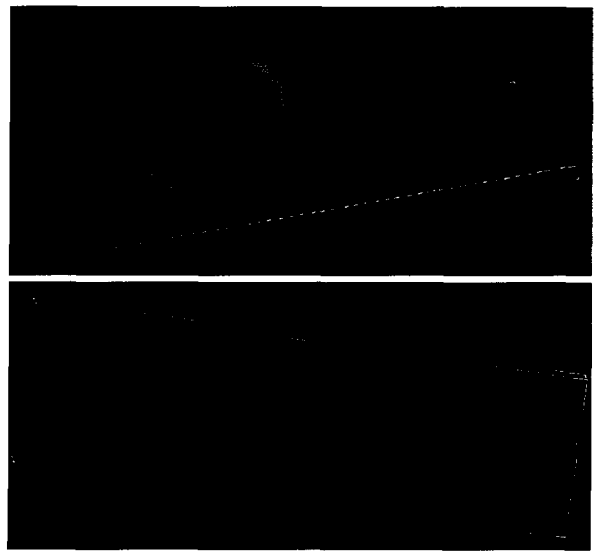

Figure 6. Hydroplaning analysis of tire.

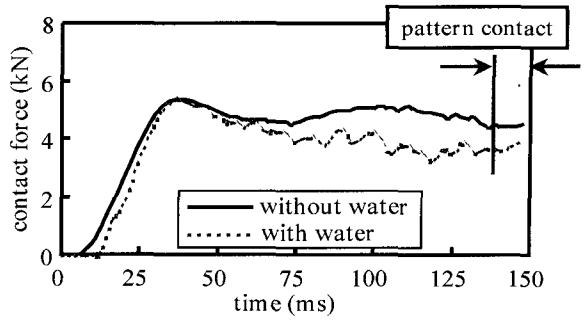

Figure 7. Time history of contact force.

water pool is 300x2000x30mm that is large enough for water flow around the footprint area, and the depth of water is 10mm. Flow boundaries around the water pool are wall boundaries through which no water can flow. The tread pattern is modeled in the part of the tread area to decrease CPU time, which is large enough for the footprint area as shown in Figure 6.

The tread pattern rolls into the water pool after the tire rolls 320 degrees. Figure 6 shows that water is drained into the two circumferential grooves and the lateral grooves.

The time histories of contact forces are shown in Figure 7. Vertical axis in this figure is the contact force between the tire and the road, and the horizontal axis is the time of the simulation in the explicit solver. The loading sequence applied to the tire model is also shown in Figure 7. A tire is inflated until 5ms and loaded until 50ms, then the blank tread area contacts with the road and the rolling motion reaches steady state until 135ms. After the steady rolling the pattern area rolls into water between 135 and 150ms. The hydrodynamic force is evaluated in this period in order to consider the effect of the tread pattern on hydroplaning.

7. VERIFICATION OF PREDICTABILITY

7.1 Comparison of Water Flow with Measurement

The flow of the drained water is shown in Figure 8 in which the tire model is removed in order to see the be havior of water clearly. The water is drained to the perimeter through the two circumferential grooves and the lateral grooves, and the bow wave is generated at the leading edge.

The water flow around the leading edge is shown in Figure 9 by lines and particles. The water is drained to the circumferential direction at the center of the contact patch and to the lateral or slantwise direction at the shoulder of the contact patch respectively. If we watch the detail of the water flow, we can recognize that the drained water flows into the circumferential grooves

Figure 8. Flow of drained water.

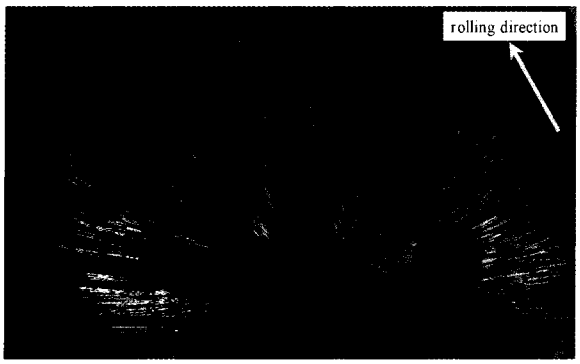

Figure 9. Water flow around the leading edge.

at the center, and flows into the lateral grooves at the shoulder. Direction of water flow is varied by the pattern geometry. This is the reason why the pattern geometry is very important for hydroplaning performance.

The comparison of the prediction and the measurement of water flow is shown in Figure 10. This photograph shows that the rolling tire in the water through the glass plate is observed. The conditions of the prediction and the experiment are the water depth of 10mm and the velocity of 60km/h. Although the viscosity of water is ignored in this simulation, the prediction of water flow is in good qualitative agreement with the measurement.

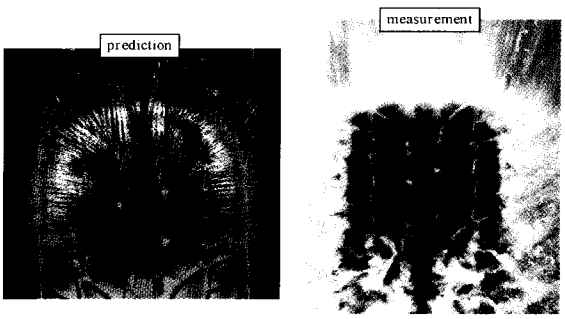

Figure 10. Comparison of prediction and measurement.

7.2. Velocity Dependence of Hydroplaning

Since hydroplaning occurs when the hydrodynamic pressure exceeds the contact pressure, the hydrodynamic force is considered as a good criterion for hydroplaning. In order to obtain the hydrodynamic force, we calculated two cases which were the rolling tires with and without water, and then we subtracted the contact force with water from that without water as shown in Figure 7. The contact force with water is smaller than that without water due to the fluid/ structure interaction, and the difference between these contact forces is considered as the hydrodynamic force in hydroplaning.

We studied the velocity dependence of the hydrodynamic force as shown in Figure 11. The hydrodynamic forces of the rolling tires, which are with tread pattern and with blank tread, increase with the velocity. Which is the same as the conventional knowledge. Furthermore Figure 12 shows that the hydro-

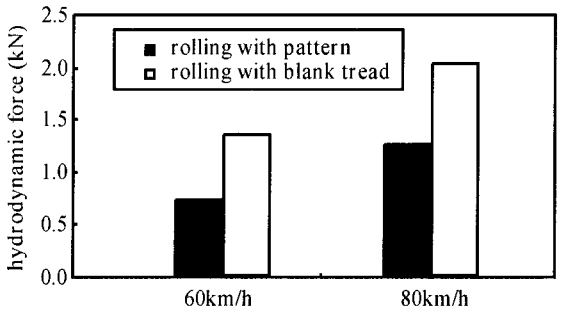

Figure 11. Velocity dependence of hydrodynamic force (1).

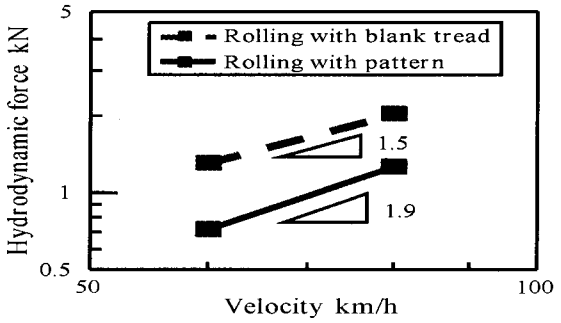

Figure 12. Velocity dependence of hydrodynamic force (2).

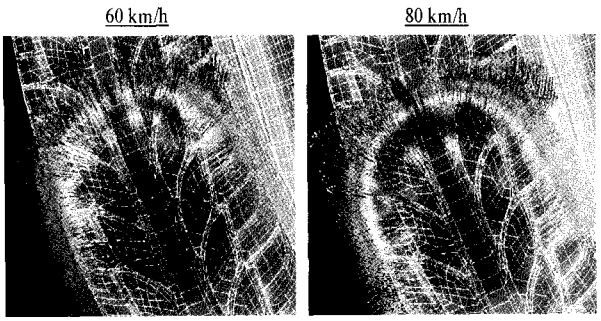

Figure 13. Water flow in different velocity.

dynamic force is almost proportional to the square of velocity both in the tire with tread pattern and with blank tread.

This corresponds to the fact that the hydroplaning velocity is proportional to the square root of the inflation pressure (Horner and Joyner, 1970).

Because the hydroplaning occurs when the hydrodynamic pressure equals the contact pressure that is almost proportional to the inflation pressure. The comparison of the water flow around the contact patch in the different velocity is shown in Figure 13. We can see that the water flow around the leading edge increases with the velocity.

7.3. Effect of Tread Pattern on Hydroplaning

The effect of the tread pattern on hydroplaning has been predicted in this study. The hydrodynamic forces with and without tread pattern are compared at 60km/h as shown in Figure 14. The tread pattern decreases the hydrodynamic force, which is the same as the conventional knowledge.

The outlines of tires at the leading edge are shown in Figure 15, which are measured at the centerline on the surface of the center rib. The outlines of both the rolling tire with tread pattern and that with blank tread are compared. The outline of the rolling tire without water in a steady state is also shown for reference. The deformation of the outlines increases with velocity, and the tread pattern decreases the deformation caused by the hydrodynamic pressure.

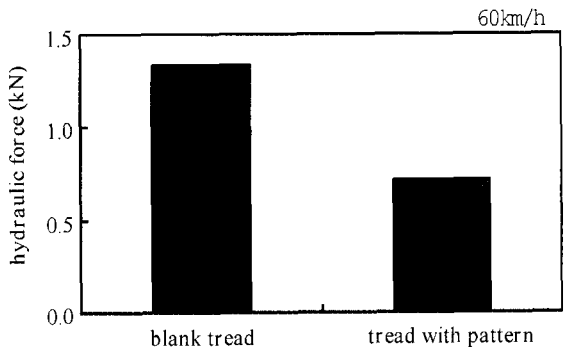

Figure 14. Hydrodynamic forces with and without tread pattern.

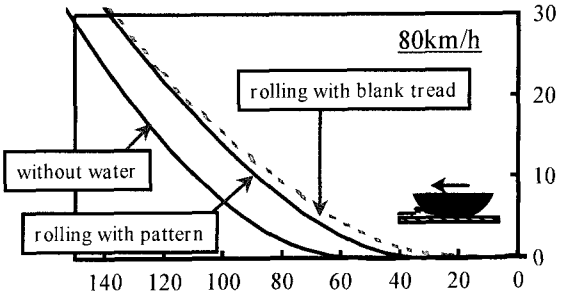

Figure 15. Deformation at the leading edge (80km/h).

8. APPLICATION TO PATTERN DESIGN

8.1. Global-Local Analysis of Water Flow for Practical Pattern Design

The hydroplaning analysis of a rolling tire needs huge CPU time, particularly in the case of a tire with practical tread pattern on the whole tire tread. So the new procedure based on the global-local analysis is developed to predict the water flow around the practical tread pattern. In the scheme of the global-local analysis as shown in Figure 16, the rolling tire with blank tread is firstly analyzed as the global analysis in which the fluid/structure interaction is considered. Then, the history of the displacement of the belt is obtained from the global analysis. After the practical pattern model is glued to the belt model, the prescribed velocities calculated from the displacement are applied to the belt in the local analysis. The local analysis is run as a separate analysis. Since the local model is more pre cise than the global model, the nodal coordinates in the local model are not necessarily the same as those in the global model. Hence the prescribed velocities in the

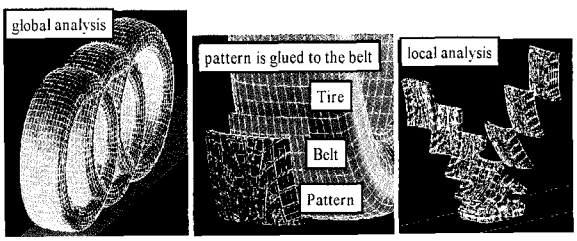

Figure 16. Global-local analysis.

local model are determined by using the element interpolation functions.

In the local analysis the fluid/structure interaction is also considered. The number of elements of the fluid domain is almost 32,000 including the coupling elements and the number of elements of the pattern part is almost 2,300 in the local analysis. Since the local model is independent of the global model, we could analyze the effect of the small change of tread pattern design on hydroplaning by using the precise model. We could also reduce the CPU time by this global-local analysis.

8.2. Development of New Pattern Design

We applied the global-local hydroplaning simulation to generate the new pattern design. In order to control the water flow around the tread pattern, we studied the three dimensional design of the block shape. Then we found that the water flow around the block tip could be made smooth by the sloped block tip as shown in Figure 17. Typical dimensions of the block tip are also indicated in Figure 17, and the depth of the tread pattern is 8mm. We call it the F1 nose because it is similar to the nose shape of the F1 car. The F1 noses are applied to the circled blocks in Figure 18.

We simulated two rolling tires that were with and without the F1 nose to study the effect on hydroplaning. The water flow of the tire with the F1 nose becomes smoother than that of the tire without the F1 nose as shown in Figure 19, which indicates that the F1 nose avoids increasing the hydrodynamic pressure around the block tip. The measurement of the tire hydroplaning velocity shows the 1 km/h improvement by the F1 so that the F1 nose is effective to improve the hydroplaning performance.

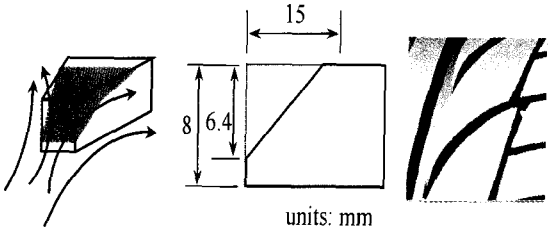

Figure 17. Shape of F1 nose.

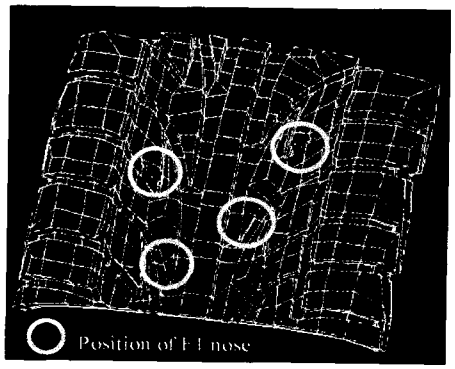

Figure 18 . Position of F1 nose.

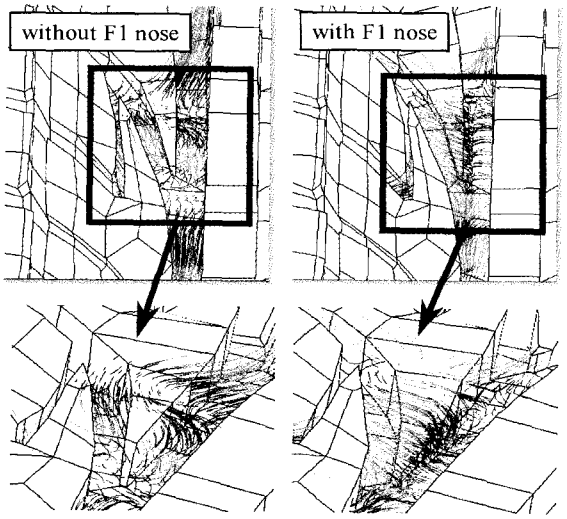

Figure 19. Water flow with and without F1 nose.

8.3. Development of Tread Pattern in Mortor Sport Tire

The hydroplaning is easily occurred in the motor sport tire due to the high speed, but the tread pattern has been designed by the trial and error process based on the designer's experience. We applied the hydroplaning simulation to design the new pattern for the racing tire, based on the design principle; make the streamline smooth.

In the beginning the simulation of a blank tread is performed, in order to see the streamline. The streamline of the front tire is asymmetric due to the camber angle, and on the other hand the streamline of the rear tire is symmetric as shown in Figure 20. The velocity is 200km/h and the water depth is 2mm.

Secondly the void geometry on the tread is designed by the streamline and the global-local analysis is used to simulate the effect of pattern. Since the streamline indicates where the water tends to flow out of the contact patch, we can effectively drain the water by grooving the void which geometry is the same as the streamline on the blank tread as shown in Figure 21. The void gradually changes from the circumferential direction in the center area to the lateral direction in shoulder area. Since the centerline of the contact area

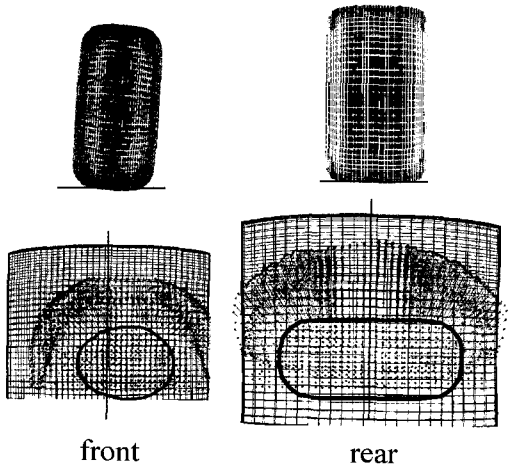

Figure 20. Streamline of tire with blank tread.

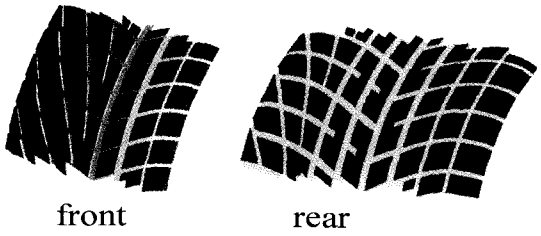

Figure 21. New pattern geometry.

is not located at the center of the tire geometry in the front tire, the void configuration becomes asymmetric. The hydrodynamic pressure is shown in Figure 22. The number in the parenthesis is the hydrodynamic force index. Judging from the decrease of the hydrodynamic force index in the new pattern, the hydroplaning performance is improved. In fact, the lap time of a tire with the new pattern was shortened in the field test.

Lastly the void geometry on the block is designed. After the water is effectively drained from the contact

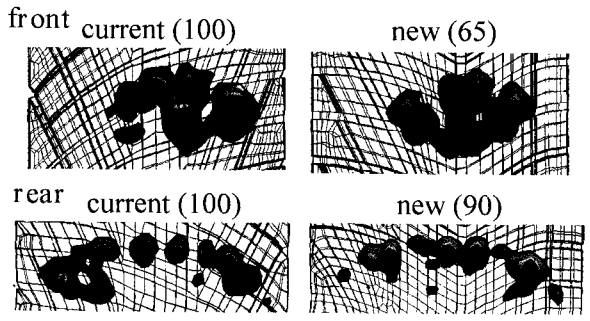

Figure 22. Comparison of current and new pattern.

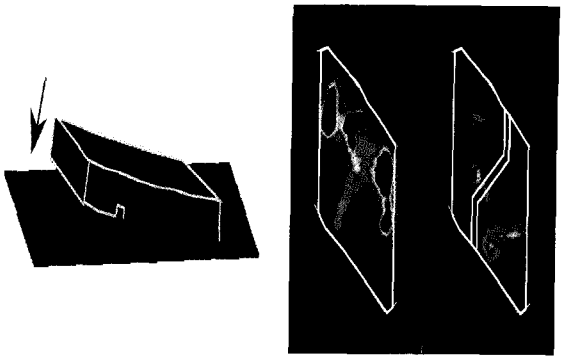

Figure 23. Effect of sipe on hydrodynamic pressure.

patch by optimizing the void geometry, we can further improve the water drainage on the block by adding the small void called the sipe. The global-local analysis is used in order to simulate the water drainage on the block as shown in Figure 23. The hydrodynamic pressure is largely reduced by adding the sipe. The lap time is also shortened by adding the sipes in the field test.

9. CONCLUSION

We established the new procedure for the hydroplaning simulation in which the following three important factors are considered; fluid/structure interaction, tire rolling, and practical tread pattern. The tire is analyzed by FEM with Lagrangian formulation and the fluid is analyzed by FVM with Eulerian formulation. Furthermore, the interface between the tire and the fluid is modeled by the general coupling function. Since the tire and the fluid can be modeled separately and their coupling is computed automatically, the complex fluid/structure interaction problems such as the hydroplaning of a tire with practical tread pattern can be analyzed practically.

We verified the hydroplaning simulation in the various parameters such as the water flow, the velocity dependence of hydroplaning, and the effect of the tread pattern on hydroplaning. We also confirmed that the hydrodynamic forces were almost proportional to square of the velocity.

We developed the new procedure based on the global-local analysis to apply the hydroplaning simulation to the design of the practical tread pattern, and we found that the three dimensional design of the block shape, which was the sloped block tip, was effective to improve hydroplaning performance. Since the hydroplaning simulation could clarify the water flow around the practical tread pattern, we could develop the new pattern in a short period based on the principle; "make the stream line smooth".

REFERENCES

Agrawall, S. K. and Henry, J. J. (1980). A simple tire deformation model for the transient aspect for hydroplaning, *Tire Science and Technology*, **8**, 23.

Albert, B. J. and Walker, J. C. (1965-66). Tyre to wet road friction., *Proc. Instn. Mech. Engrsn*,**180**, 105.

Allbert, B. J. (1968). Tires and hydroplaning, *SAE paper* 680140.

Boness, R. J. (1968). A theoretical treatment of the aquaplaning tyre, *Automobile Engineer*, 260.

Browne, A., Cheng, H., and Kistler, A. (1972). Dynamic hydroplaning of pneumatic tires, *Wear*, **20**, 1.

Browne, A. L. (1977a). Computer-aided prediction of the effect of tire tread pattern design on thick film wet traction, *GMR-2487*.

Browne, A. L. (1977b). *Tire Science and Technology* **5**, 6.

Browne, A. L. and Whicker, D. (1977). Design of thin tread elements for optimum thin film wet traction, *SAE paper* 770278.

Browne, A. L., Whicker, D., and Rohde, S. M. (1975). Predicting the effect of tire tread pattern design on thick film wet traction, *Tire Science and Technolog*, **3**, 215.

Browne, A. L. (1975). Tire deformation during dynamic hydroplaning, *Tire Science and Technology*, **3**, 16.

Grogger, H. and Weiss, M. (1996). Calculation of the three-dimensional free surface flow around an automobile tire, *Tire Science and Technology*, **24**, 39.

Grogger, H. and Weiss, M. (1997). Calculation of the hydroplaning of a deformable smooth-shaped and longitudinally-gooved tire, *Tire Science and Technology*, **25**, 265.

Hays, D. F. and Browne A. L. eds. (1974). *The Physics for Tire Traction—Theory and Experiment*- Plenum Press, 281-297.

Horner, W. B. and Joyner. (1970). U. T. pneumatic tire hydroplaning and some effects on vehicle Performance, *SAE paper* 970C.

Moore, D. F. (1964). On the inclined non-inertial sinkage of a flat plate, *J. Fluid Mech*, **20**, 321.

Moore, D. F. (1965). A review of squeeze films, *Wear*, **8**, 245.

Moore, D. F. (1967). A Theory of Viscous Hydroplaning. *Int.J.Mech.Sci* **9**, 797.

Moore, D. F. (1975). *The Friction of Pneumatic Tyres*, Elsevier Scientific Publishing Company, 103–113.

MSC. Dytran USER'S MANUAL.

Okamura, M., Someya, T. (1977). Research of hydro-planing(1). (in Japanese), *JSME*, **43**, 3932.

Okamura, M., Someya, T. (1977). Research of hydro-planing(2). (in Japanese), *JSME*, **43**, 3944.

Rohde, S. M. (1977). On the combined effects of tread element flexibility and pavement microstructure on thin film wet traction, *SAE paper* 770277.

Sakai, H. (1987). *Tire Technology (in Japanese)*, Grand Prix Publication, 271.

Sakai, H., Kanaya, O., and Okuyama, T. (1978). The effect of hydroplaning on the dynamic characteristics of car, truck and bus tires, *SAE paper* 780195.

Whicker, D., Browne, A. L., and Rohde, S. M. (1976). Some effect of inclination on elastohydrodynamic squeeze film problems, *J. Fluid Mech*, **8**, 247.

Yagita, M., et al. (1996). Effects of a ground plate on magnus effect of a rotating cylinder (in Japanese), *JSME*, B**62**: 1294.

Yeager, R. W. and Tuttle, J. L. (1972). Testing and analysis of tire hydroplaning, *SAE paper* 720471.